Colloid and Polymer Science (2018) 296:1249–1257
https://doi.org/10.1007/s00396-018-4342-7

ORIGINAL CONTRIBUTION

A novel oligo-pyrazole-based thin film: synthesis, characterization, optical and morphological properties

Adnan Cetin[1] · Adem Korkmaz[2] · Ishak Bildirici[3]

Received: 5 April 2018 / Revised: 11 May 2018 / Accepted: 14 May 2018 / Published online: 5 June 2018
© The Author(s) 2018

Abstract

Pyrazole-3,4-dicarboxylic acid **2** was synthesized via the hydrolysis of pyrazole-3-carboxylic acid **1** and subsequently heated with thionyl chloride to give the novel pyrazole-3,4-dicarbonyl dichloride **3**, which was easily converted into oligo-pyrazole **4** upon its reaction with *p*-phenylene-diamine. These newly synthesized compounds were characterized by ^{1}H-NMR, ^{13}C-NMR, and FT-IR spectroscopy, and gel permission chromatography (GPC). Three novel oligo-pyrazole thin films were prepared using oligo-pyrazole **4** with these respective values of thickness: 20, 21, and 24 μm. The optical properties of the films, including the absorbance, transmittance, and optical band gap, were determined using UV-vis spectroscopy. The E_g values of the films were found to be 1.426, 1.537, and 1.648 eV for the 20, 21, and 24 μm thick organic films, respectively. Atomic force microscopy (AFM) was used to examine the surface morphology and properties of the organic films. In the AFM images, a few black regions were observed and several yellow regions appeared over a large area, and the surface of the oligo-pyrazole films had an extremely low roughness value. The as-synthesized oligo-pyrazole has great potential in optoelectronic applications according to the optical properties of the as-prepared films.

Keywords Absorbance · Conjugated polymer · Organic semiconductor · Pyrazole · Thin film

Introduction

Conjugated polymers are important target molecules for synthetic chemists due to their use in solar cells, organic photovoltaics, organic light emitting diodes, and thin film transistors, as well as their industrial applications [1–3]. The search for new materials depends on the rapid development of science and technology, which has created an intense area of research on conducting polymers and increased the importance of the projects in this area. Recently, the synthesis of new polyamide derivatives has become an increasingly popular topic and widely studied research area [4–6]. In particular, their optical properties and physicochemical properties have guided researchers towards the synthesis of polyamide derivatives using existing methods and applications [7, 8].

Poly-pyrazoles are an important class of heterocyclic polymers, which have become more popular than before due to their wide range of properties such as film formation and high thermal stability [9, 10]. Poly-pyrazoles and pyrazoles have also been successfully applied in many fields including biology, industry, and pharmaceutical chemistry [11–13]. Past studies used conjugated polyamides (e.g., amide groups) for drug delivery in medicine [14, 15]. Furthermore, poly-pyrazoles and pyrazoles have many advantages in several application fields such as optics and optoelectronic technology [9, 16].

Highlights
- A new different asymmetric oligo-pyrazole is synthesized and its thin films were prepared.
- The optical properties of thin films were investigated.
- The prepared thin films can be a candidate as a semiconductor due to having the optical band gap (E_g) values (1.426, 1.537, and 1.648 eV).

Electronic supplementary material The online version of this article (https://doi.org/10.1007/s00396-018-4342-7) contains supplementary material, which is available to authorized users.

✉ Adnan Cetin
adnankimya@gmail.com

[1] Faculty of Education, Department of Science, Muş Alparslan University, Muş, Turkey

[2] School of Health, Muş Alparslan University, Muş, Turkey

[3] Faculty of Pharmacy Department of Pharmaceutical Chemistry, Yüzüncü Yıl University, Van, Turkey

One of the most common applications of polymer materials is in thin film devices. Thin films that are made of these polymers have several advantages when used as optical coatings, coatings in electronics, and decorative protective coatings, thanks to the fundamental characteristics they have. For instance, optical, mechanical, and electrical properties are significantly increased when polymer materials are used as a thin film [17, 18]. In particular, thin films have been used in the construction of semiconductors and superconducting devices, insulation and transmission coatings, and circuits due to their electrical properties. They are also used in reflective and non-reflective coatings, interference filters, and optical discs due to their optical properties. In addition, thin films are used in memory disks due to their magnetic properties [19, 20].

This study aimed to synthesize different oligo-pyrazole-based thin films that are newly developed and to investigate their optical properties such as the optical band gap and transmittance. Furthermore, the study determined the surface morphology of the new thin film (21 μm) that had different thickness levels using atomic force microscopy (AFM).

Experimental

Materials and equipment

All reagents and solvents were purchased from Merck, Sigma and Aldrich companies. These materials were used without purification. Infrared spectra were recorded on a Shimadzu IR-470 spectrophotometer. ^{1}H (400 MHz) and ^{13}C (100 MHz) NMR spectra were recorded on a Bruker DRX-400 high-performance digital FT-NMR spectrometer. NMR spectra were obtained in solutions of deuterated chloroform. Molecular weight and PDI of the synthesized oligo-pyrazole were determined by gel permeation chromatography (GPC) using Agilent 1100 Series, equipped with refractive index detector. Optical measurements of thin films at different thicknesses were carried out with a Shimadzu model UV-1800 spectrophotometer in the wavelength range of 1100–190 nm at room temperature. An Ambios Q-Scope AFM device was used to study the surface structures of the films.

1-(3,4-Dimethylphenyl)-4-(ethoxycarbonyl) -5-phenyl-1*H*-pyrazole-3-carboxylic acid (1)

To synthesize compound **1**, procedure existed in literature was followed [21]. The yield of **1** was 75%; mp 163.02 °C.

1-(3,4-Dimethylphenyl) -5-phenyl-1*H*-pyrazole-3,4-dicarboxylic acid (2)

Compound **1** (0.364 g, 1 mmol) was heated in solution of sodium hydroxide (0.1 g 2.5 mmol) in 20 mL water for 1 h. The solution was cooled down to room temperature. It was added with concentrated hydrochloric acid (1.5 mL) and water (1.5 mL). The white solid product was occurred. It was filtered and it was washed with water. Yield 90%. Color white. mp 126–128 °C. FT-IR (ν, cm^{-1}) 3350 (br, -OH), 3064 (aromatic C-H), 2936 (aliph. C-H), 1721–1710 (C=O, acide), ^{1}H NMR (400 MHz, $CDCl_3$) δ (ppm) 11.6 (*br.s*, 2H, -OH), 8.1 (m, 1H), 7.9 (m, 2H), 7.6 (m, 2H), 7.1 (m, 3H), 2.1 (s, 3H, Ar-CH_3), 1.8 (s, 3H, Ar-CH_3). ^{13}C NMR (100 MHz, $CDCl_3$) δ (ppm) 171.3, 167.9 (C=O, acid), 145.2 (C_3), 142.1 (C_5), 135.0, 134.0, 132.9, 132.8, 132.0, 128.0, 127.2, 125.0, 115.8, 115.7 (C_4), 29.4 (Ar-CH_3), 20.7 (Ar-CH_3). (+)ESI-HRMS *m*/*z* calculated for [$C_{19}H_{16}N_2O_4 + H^+$] 337.3562; observed 337.3565.

1-(3,4-Dimethylphenyl) -5-phenyl-1*H*-pyrazole-3,4-dicarbonyl dichloride (3)

Compound 2 (0.397 g, 1 mmol) was added to the reaction flask that included excessive thionyl chloride and refluxed at 80 °C. After 6 h, the reaction mixture, which dissolved over time, was cooled down to room temperature. Excessive thionyl chloride was evaporated. The remaining oily product was purified in dry ether and then was crystallized from toluene, to yield 75%. Color milk white. FT-IR (ν, cm^{-1}) 3062 (aromatic C-H), 2928 (aliph. C-H), 1720, 1700 (C=O, acyl), ^{1}H NMR (400 MHz, $CDCl_3$) δ (ppm) 8.0 (s, 1H), 7.8 (s, 1H), 7.6 (m, 2H), 7.4 (m, 2H), 7.2 (m, 2H), 2.6 (s, 3H, Ar-CH_3), 2.1 (s, 3H, Ar-CH_3). ^{13}C NMR (100 MHz, $CDCl_3$) δ (ppm) 171.0, 167.5 (C=O, acyl), 142.3 (C_3), 141.8 (C_5), 135.6, 133.6, 133.0, 132.4, 130.5, 130.1, 128.4, 128.1, 127.7, 126.3, 114.1 (C_4), 30.8(Ar-CH_3), 22.8 (Ar-CH_3). (+)ESI-HRMS *m*/*z* calculated for [$C_{19}H_{14}Cl_2N_2O_2 + H^+$] 374.2438, observed 374.2439.

Synthesis of poly(p-phenylene-1-(3,4-dimethylphenyl) -5-phenyl-1*H*-pyrazole-3,4-dicarboxyamide (4)

Pyrazole-3,4-dicarbonyl dichloride **3** (0.08 g 0.25 mmol) was dissolved in anhydrous tetrahydrofuran (10 ml). The *p*-phenylene-diamine (0.028 g 0.25 mmol) was added to the reaction pot and the mixture was refluxed for 24 h under an atmosphere of nitrogen. Then, it was cooled to room temperature. The solvent was evaporated. The precipitated product was washed with diethyl ether. Then, it was filtered and dried. Yield 80%. Color brown. FT-IR (ν, cm^{-1}) 3385 (N-H, amide), 2967 (aromatic -CH), 1731 (C=O, acyl), 1652 (C=O, amide), 1595–1579 (C=N), 1536–1449 (aromatic, C=C), 1313 (C-N). ^{1}H NMR (400 MHz, $CDCl_3$) δ (ppm) 8.7, 8.4 (-NH, amide), 7.9–6.3 (m, Ar-H), 4.4 (-NH, aromatic), 2.5, 2.2, 2.1, 2.0, 1.7 (s, Ar-CH_3). ^{13}C NMR (400 MHz, $CDCl_3$) δ (ppm) 172.5, 165.8, 162.3, 159.9 (-C=O), 149.8 (C_3), 142.1 (C_5), 140.6,

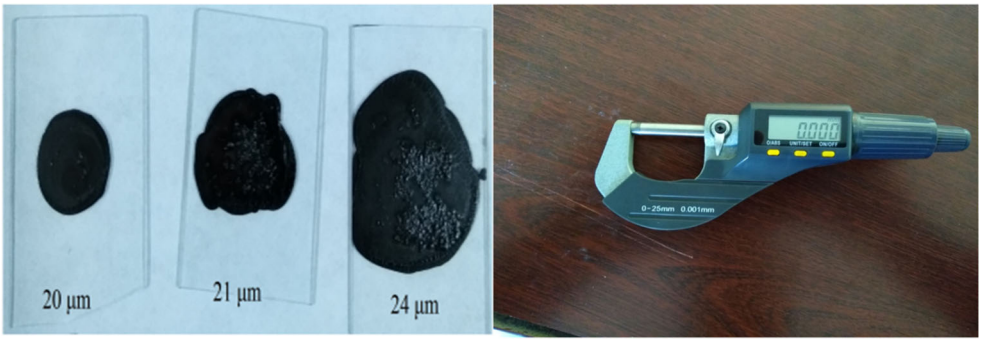

Fig. 1 Images of the thin films of oligo-pyrazole with thickness values of 20, 21, and 24 μm

139.6, 139.3, 139.2, 134.5, 130.4, 130.2, 130.1, 129.4, 127.2, 123.1, 121.7, 117.5, 114.1, 111.3, 110.3, 108.3 (C_4·), 30.9, 30.3, 22.4, 22.7, 21.5 (Ar-CH_3). *M*n = 1333 g/mol, Mw = 2347 g/mol, (polydispersity index, PDI, 1.872).

Preparation of the thin films that synthesized oligo-pyrazole (4)

Oligo-pyrazole **4** (0.05 g) was added to 1 mL of DMF and the resulting solution was stirred at room temperature for 1 h. Any insoluble oligo-pyrazole was removed by filtration. The surface of a glass substrate was cleaned using piranha solution (sulfuric acid and hydrogen peroxide) and then rinsed with water. The solution of oligo-pyrazole was added dropwise on the glass substrate and left to dry to form a thin film of oligo-pyrazole **4**. To obtain films with different thickness levels, the process was repeated several times for each film. Using this method, three films with thickness values of 20, 21, and 24 μm were obtained. The thickness values of the films were measured using a micrometer (sensitivity = 0.001 mm), as shown in Fig. 1.

Results and discussion

Synthesis and characterization

Poly-pyrazoles are the most extensively studied subject in polymer chemistry and organic chemistry because of their reliability, accessibility, and chemo-selectivity. Pyrazole-3-carboxylic acid **1** was synthesized according to a literature procedure [21] and pyrazole-3,4-dicarboxylic acid **2** was obtained from the basic hydrolysis of **1** (Scheme 1). The structure of **2** was confirmed using NMR spectroscopy by the two carboxylic acid proton signals at $\delta = 11.68$ ppm and the two carbonyl carbon signals at $\delta = 171.3$ and δ 167.9 ppm, and using FT-IR spectroscopy by the characteristic IR absorption bands at 3350 cm^{-1} (COOH), 3064 cm^{-1} (Ar-C-H), 1721 and 1710 cm^{-1} (acid, C=O).

The monomeric starting material, pyrazole-3,4-dicarbonyl dichloride **3**, was prepared upon heating **2** with excess thionyl chloride. All the new compounds (**1**–**3**) were confirmed using spectroscopic methods, which were consistent with the previous studies [22]. The preparation of oligo-pyrazole was performed using the one-step procedure shown in Scheme 1. Poly(p-phenylene-1-(3,4-dimethylphenyl)-5-phenyl-1H-pyrazole-3,4-dicarboxyamide **4** was synthesized upon the reaction of **3** and *p*-phenylene-diamine in refluxing THF for 1 day under an atmosphere of argon gas. The average molecular weight (*Mn*), average molecular weight (*Mw*), and polydispersity index (PDI) of the as-synthesized oligo-pyrazole **4** were determined by GPC using poly(methyl methacrylate). The Mn, Mw, and PDI of the as-synthesized oligo-pyrazole were observed to be 1333, 2347, and 1.872 g mol^{-1}, respectively. As shown Scheme 1, the as-synthesized oligo-pyrazole **4** was determined be a trimeric structure using gel permeation chromatography. The as-synthesized oligo-pyrazole **4** has three pyrazole structural units and ten phenyl groups. In addition, the as-obtained oligo-pyrazole was asymmetric due to the structure of the monomer. The better conjugation was used as a warranty since there were many aromatic structures. This also explains the low optical band gap value.

The structure of the as-obtained oligo-pyrazole was also confirmed by the FT-IR, ^{1}H NMR, and ^{13}C NMR spectra.

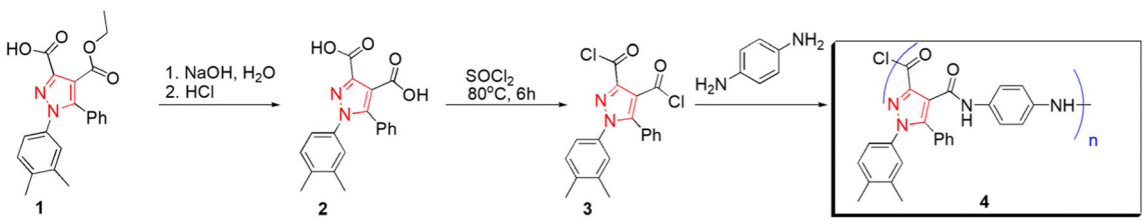

Scheme 1 The synthesis of oligo-pyrazole **4**

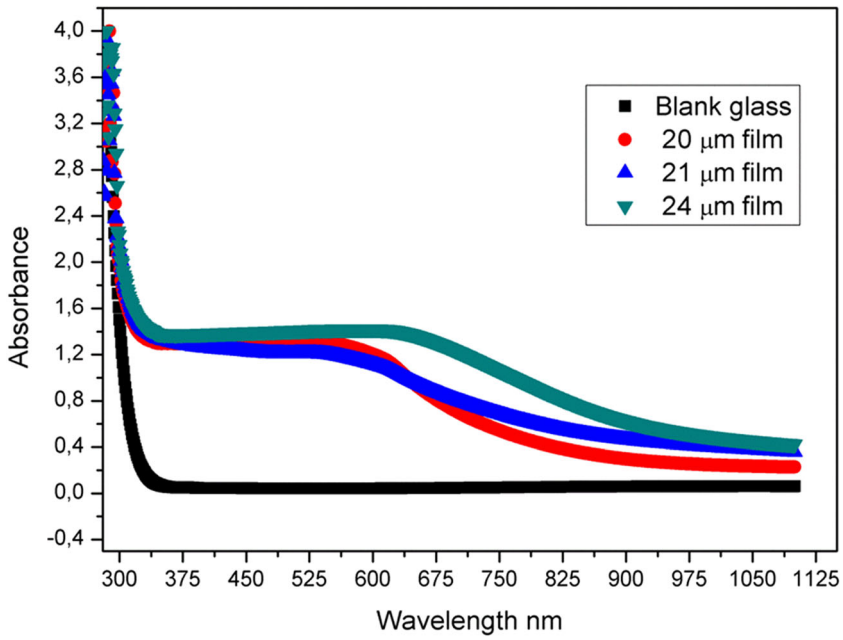

Fig. 2 The graph of absorbance vs wavelength obtained for the oligo-pyrazole-coated and uncoated glass samples

The FT-IR bands at 3385 cm^{-1} correspond to the -NH amide groups. The bands corresponding to the amide (C=O) groups appear in the region of 1652–1731 cm^{-1}. The band observed at 3066 cm^{-1} was attributed to the aromatic C-H stretching vibrations. The strong bands at 1595 and 1579 cm^{-1} correspond to the C-C stretching of the phenyl rings. In the case of the as-synthesized oligo-pyrazole **4**, the correct structure was established by ^{1}H NMR and ^{13}C NMR spectroscopy in which the characteristic peak for the C=NH proton in was observed at $\delta = 9.94$ ppm and the NH protons were observed as singlet peaks at $\delta = 6.0$ and 5.1 ppm, and as multiplets in the region of $\delta = 6.9$–8.0 due to the aromatic protons in the as-synthesized oligo-pyrazole **4**.

The optical properties of the thin films

The absorbance curves recorded for the oligo-pyrazole coated glass samples and uncoated blank glass were recorded and shown in Fig. 2. The absorbance value of the oligo-pyrazole coated glass samples was increased when compared to the blank glass sample [23]. This effect was easily observed at all the wavelengths studied. In particular, the absorption between 550 and 900 nm increased sharply. An increase in the absorbance value was also observed for the thin films with different thickness levels.

The increase in absorbance could be greater if the oligo-pyrazole film was thick. The highest absorbance value was

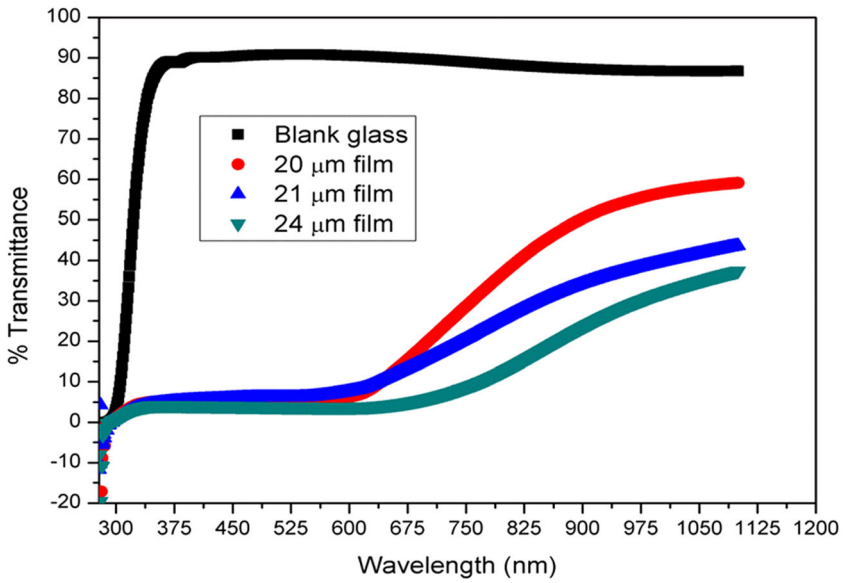

Fig. 3 The graph of transmittance vs wavelength obtained for the oligo-pyrazole-coated and uncoated glass samples

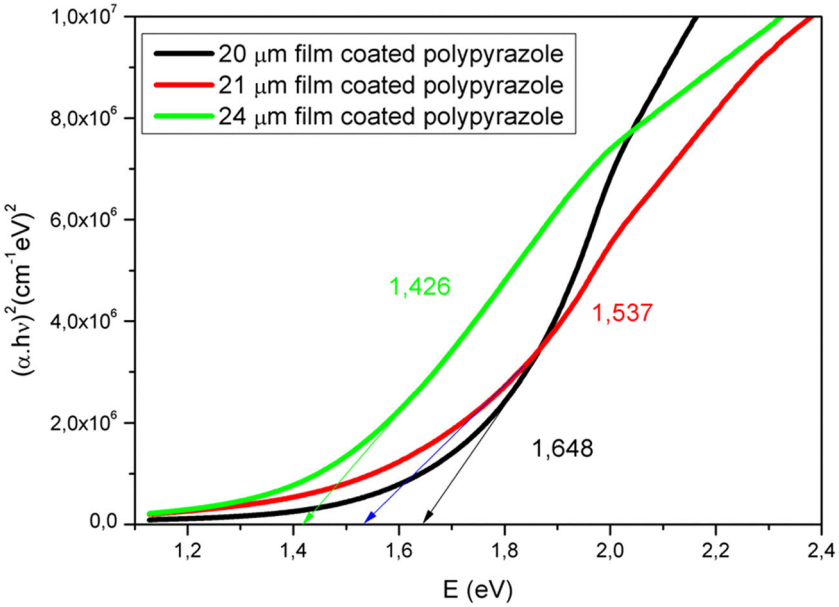

Fig. 4 The graph of $(\alpha h\nu)^2$ vs photon energy obtained for oligo-pyrazole

observed for the 24 μm film, while the lowest absorbance value was observed for the 20 μm film. The transmittance graph obtained for the 20, 21, and 24 μm films is shown in Fig. 3.

After coating the glass substrate with oligo-pyrazole, the transmittance was significantly reduced. The transmittance value of the blank glass sample was in the range of 90–100% (Fig. 3). Upon coating the glass substrate with oligo-pyrazole, the transmittance value was at most 55%. The transmittance value for the oligo-pyrazole-coated films remained constant in the range of 300–550 nm, whereas it increased in the range of 550–1100 nm. The average transmittance values of the 20, 21, and 24 μm oligo-pyrazole films were 26, 19, and 13% between 294 and 1100 nm, respectively. The average transmittance values of the same films were calculated 12, 10, and 5% in the visible range (between 380 and 780 nm), also respectively. As a result, the transmittance value decreased after increasing the film thickness [24]. Also, we can say that the transparent quality of the oligo-pyrazole films is very low in the visible region due to the remarkably low light transmission [25]. One of the most important parameters for the optical properties of a film coating is the *Eg* value. The photon energy vs $(\alpha.h\nu)^2$ plot was used to obtain the direct band gap of oligo-pyrazole using the Tauc equation (Fig. 4) [26].

As shown in Fig. 4, the E_g values observed for the films with thickness values of 20, 21, and 24 μm were 1.646, 1.537, and 1.428 eV, respectively. The E_g value decreased upon

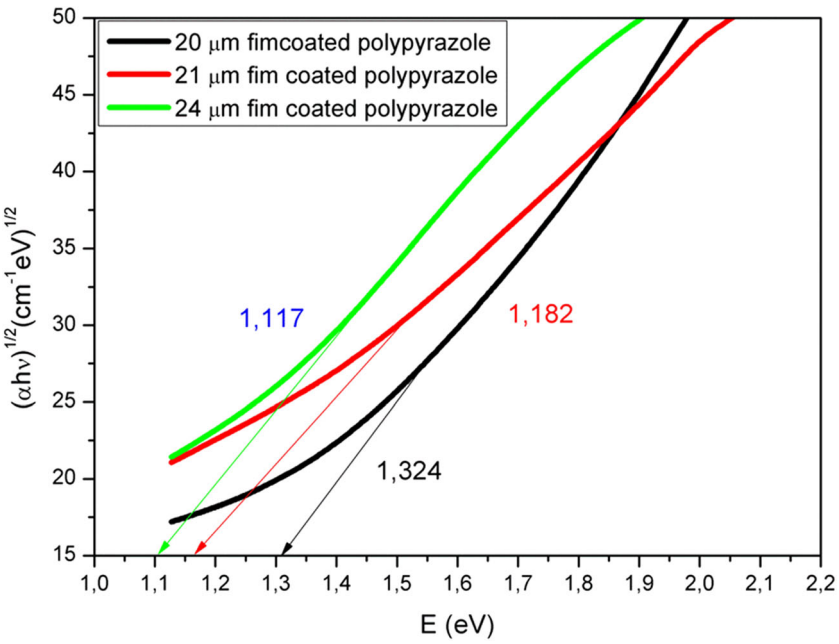

Fig. 5 The graph of $(\alpha h\nu)^{1/2}$ vs photon energy obtained for the thin films of oligo-pyrazole

Table 1 The E_g values obtained for the oligo-pyrazole films with thickness values of 20, 21, and 24 μm

No	Thickness (μm)	Direct E_g values (eV)	Indirect E_g values (eV)	Forbidden indirect Eg values (eV)
1	20	1648	1324	1466
2	21	1537	1182	1339
3	24	1426	1117	1145

increasing the thickness of the oligo-pyrazole film and it was possible to further reduce the E_g value by increasing the film thickness further. In addition, the E_g value of the newly synthesized oligo-pyrazole was very low. When the coated oligo-pyrazole film is set to the desired thickness, it acts as the semiconducting material [27]. Obviously, the desired E_g value can be obtained for a particular optical application by adjusting the film thickness. The photon energy vs $(\alpha.h\nu)^2$ plot was used to determine the indirect E_g values for the thin films of oligo-pyrazole (Fig. 5).

The indirect band gap values observed for the films with thickness values of 20, 21, and 24 μm were found to be 1.324, 1.182, and 1.117 eV, respectively. The E_g value decreased after increasing the film thickness (Fig. 5). The direct transition was sharper than the indirect transition (Figs. 4 and 5) and the direct transition was more dominant than the indirect transition. The direct E_g and indirect E_g values observed for the oligo-pyrazole films with different thickness levels are shown in Table 1.

The graph of E (eV) vs $(\alpha h\nu)^{1/3}$ was plotted for the oligo-pyrazole films with thickness values of 20, 21, and 24 μm (Fig. 6). The forbidden indirect band gap values observed for the 20, 21, and 24 μm films were 1.466, 1.339, and 1.145 eV, respectively. The forbidden indirect band gap value decreased after increasing the film thickness.

The optical band gap is an important parameter for semiconductors. It particularly has a shifting effect in the design of semiconductor materials [28]. For this reason, it is very important that these materials may be modeled and have the desired optical energy gap value. Also, organic photovoltaic devices are among the most popular research areas, because the organic molecules used in these devices have certain properties that are superior to photovoltaic applications. These properties include being low cost, flexible, light weight, and suitable for many new designs [29, 30]. The oligo-pyrazole compound has a very low band gap value, although the repeating unit numbers were very small. This low value (1.42–1.64 eV) is desirable for photovoltaic applications [31]. The minimum band gap value of organic materials that were studied in photovoltaic applications was 1.6–2.2 eV [32, 33]. It appears that the oligo-pyrazole compound has a low Eg value as the polymers used in photovoltaic applications. Thus, the synthesized oligo-pyrazole molecule has a potential to be used in photovoltaic applications. The oligo-pyrazole molecule increases the thermal stability by lowering the internal energy because it shows high conjugation [34].

The surface morphology of thin film

In this study, AFM was used to investigate the surface properties of the oligo-pyrazole thin films. Two- and three-dimensional images (9 μm × 9 μm) of the surface morphologies of the thin films deposited on the glass substrate were recorded at a scanning speed of 0.7 Hz using the AFM device in non-contact mode [35]. The surface features, such as the surface roughness, skewness, kurtosis, and height, were determined using the software on the AFM instrument. Figure 7 shows the two-dimensional and three-dimensional AFM image of the oligo-pyrazole thin film 21 μm coated on a glass

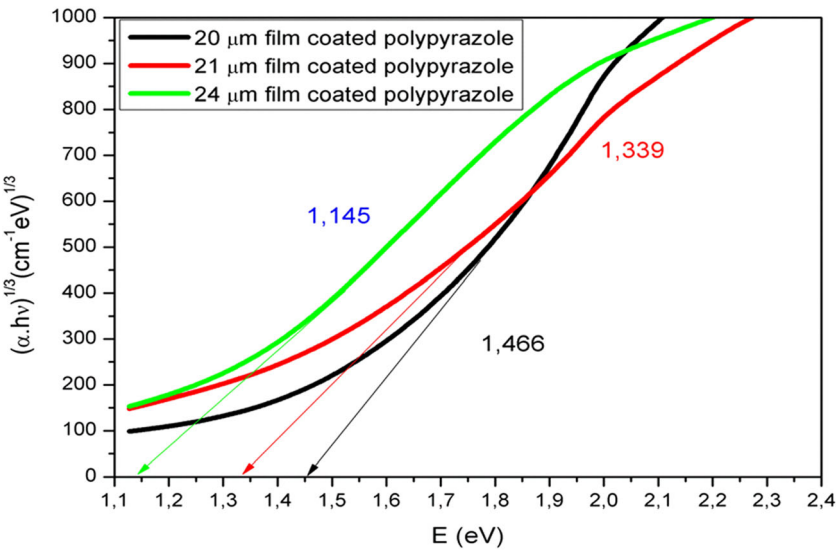

Fig. 6 The graph of $(\alpha h\nu)^{1/3}$ vs photon energy obtained for the thin films of oligo-pyrazole

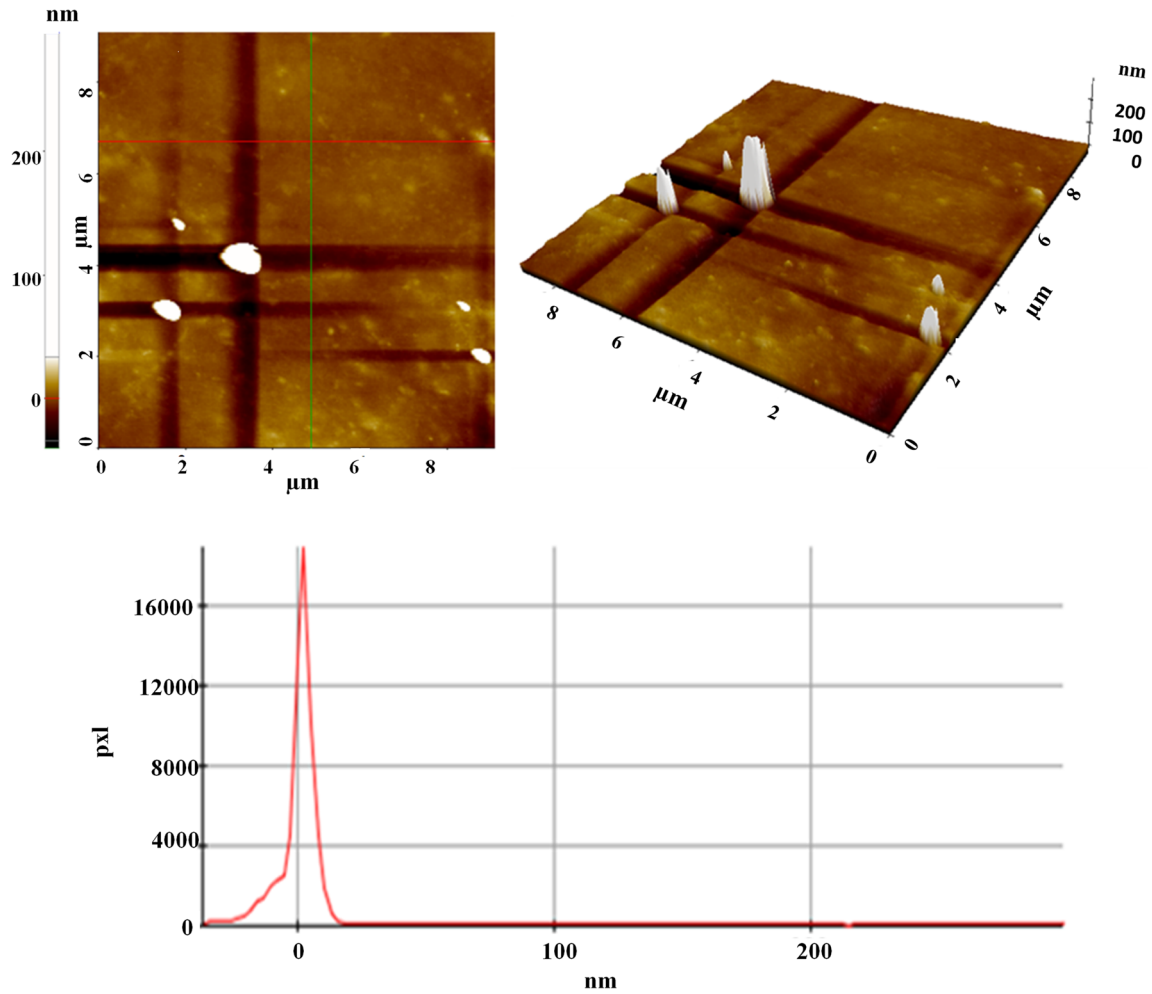

Fig. 7 The 2D and 3D AFM images of the as-synthesized oligo-pyrazole thin film coated on a glass substrate

substrate [36, 37]. In the AFM images, a few black regions and several yellow regions appeared over a large area. The surface properties of the films were analyzed using high-resolution AFM imaging and image processing evaluation software. The AFM surface analysis results obtained for the thin film coated on the glass substrate showed the average surface roughness, which gives the deviation in height, was 3.34 nm; the average square root roughness, which represents the standard deviation of the surface height, was 5.65 nm and the skewness, which represents the symmetry, was − 0.26 nm. The Kurtosis value, which is a measure of pressure, was 8.84 nm. The total roughness, which is the sum of the maximum height and the maximum depth for the entire measurement length, was 43.80 nm for the red line in the 2D-AFM image, average surface roughness (3.90 nm), average square root roughness (5.74 nm), and skewness (1.18). The Kurtosis value was 5.43. The total roughness was 33.79 nm for the green line in the 2D-AFM graph, as shown in Fig. 6. The skewness value in the produced film was negative for the red line, which showed that the pits on the film surface were more dominant than the peaks.

The height distribution graph was obtained using the AFM tool (Fig. 7). The height distribution plot is associated with the homogeneous grain distribution observed on the samples' surface. The thin film coated on the glass substrate exhibits a perfect Gauss curve [38]. To summarize, three thin films were obtained with different thickness levels and their optical properties were examined. Desired optical properties can be achieved by adjusting the oligo-pyrazole film thickness.

Conclusions

This study synthesized a novel conjugated oligomer that was comprised of pyrazole skeleton. Thin films made from this oligomer with different thickness (20, 21, and 24 µm) were prepared and their optical properties were investigated. The band gap values of the oligo-pyrazole films were very low (1.426, 1.537, and 1.648 eV, respectively) and were suitable for optical applications. Furthermore, the band gap value was observed to decrease after increasing the thickness of the thin film, which showed that their

optical applications could be controlled by adjusting the oligo-pyrazole film thickness in order to adjust the desired band gap. AFM was used to examine the surface morphology and properties of the organic films, and the two-dimensional and three-dimensional AFM images were used to see the gaps on the surface of the samples. The surfaces of the oligo-pyrazole films have extremely low roughness values. The as-prepared films exhibit good surface morphologies that are suitable for optoelectronic applications.

Acknowledgements The authors thank Dr. Erman Erdoğan and Dr. Arif Kösemen who helped in interpreting AFM analysis work.

Funding information This study received partially financial support from the Mus Alparslan University (BAYPUAM) (Grant No. MSÜ14-EMF-G05).

Compliance with ethical standards

Conflict of interest The authors declare that they have no conflict of interest.

Open Access This article is distributed under the terms of the Creative Commons Attribution 4.0 International License (http://creativecommons.org/licenses/by/4.0/), which permits unrestricted use, distribution, and reproduction in any medium, provided you give appropriate credit to the original author(s) and the source, provide a link to the Creative Commons license, and indicate if changes were made.

References

1. Bundgaard E, Krebs FC (2007) Sol Energ Mat Sol C 91(11):954–985.
2. Yao H, Chen Y, Qin Y, Yu R, Cui Y, Yang B, Hou J (2016) Design and synthesis of a low bandgap small molecule acceptor for efficient polymer solar cells. Adv Mater 28:8283–8287
3. Cetin A, Korkmaz A, Kaya E (2018) Synthesis, characterization and optical studies of conjugated Schiff base polymer containing thieno[3,2- b]thiophene and 1,2,4-triazole groups. Opt Mater 76: 75–80
4. Kausar A (2018) Composite coatings of polyamide/graphene: microstructure, mechanical, thermal, and barrier properties. Compos Interface 25(2):109–125
5. Park SJ, Choi W, Nam SE, Hong S, Lee JS, Lee JH (2017) Fabrication of polyamide thin film composite reverse osmosis membranes via support-free interfacial polymerization. J Membr Sci 526:52–59
6. Kausar A (2017) State-of-the-Art overview on polymer/POSS nanocomposite. Polym Plast Technol Eng 56:1401–1420
7. Lee JS, Seo JA, Lee HH, Jeong SK, Park HS, Min BR (2017) Simple method for preparing thin film composite polyamide nanofiltration membrane based on hydrophobic polyvinylidene fluoride support membrane. Thin Solid Films 624:136–143
8. Khorshidi B, Thundat T, Fleck BA, Sadrzadeh M (2016) A novel approach toward fabrication of high performance thin film composite polyamide membranes. Sci Rep 6:22069
9. Cetin A, Gündüz B, Menges N, Bildirici I (2017) Unsymmetrical pyrazole-based new semiconductor oligomer: synthesis and optical properties. Polym Bull 74:2593–2604
10. Mukundam V, Kumar A, Dhanunjayarao K, Ravi A, Peruncheralathan S, Venkatasubbaiah K (2015) Tetraaryl pyrazole polymers: versatile synthesis, aggregation induced emission enhancement and detection of explosives. Polym Chem 6:7764–7770
11. Yang B, Wang Y, Xiao L, Hu X, Zhou G (2017) Enhanced antibacterial effect of polypyrazole-graphene oxide composite. Macromol Res 25:21–26
12. Camurlu P, Gültekin C, Gürbulak V (2013) Optoelectronic properties and electrochromic device application of novel pyrazole based conducting polymers. J Macromol Sci A 50:588–595
13. Giornal F, Pazenok S, Rodefeld L, Lui N, Vors JP, Leroux FR (2013) Synthesis of diversely fluorinated pyrazoles as novel active agrochemical ingredients. J Fluor Chem 152:2–11
14. Abdel-Halim AH (2017). Eur J Med Chem 134:392
15. Park SB, Lih E, Park KS, Joung YK, Han DK (2017) Biopolymer-based functional composites for medical applications. Prog Polym Sci 68:77–105
16. Carlson WB, Phelan GD (2013) U.S. patent no. 20160200845A1. Washington, DC: U.S. Patent and Trademark Office
17. Martin BD, Leary DH, Trammell SA, Ellis GA, Naciri J, Depriest JC, Deschamps JR (2015) One-step synthesis of a new photoelectron-accepting, n-dopable oligo(pyrazole). Synth Met 204:32–38
18. Bucella SG, Luzio A, Gann E, Thomsen L, McNeill CR, Pace G, Caironi M (2015) Macroscopic and high-throughput printing of aligned nanostructured polymer semiconductors for MHz large-area electronics. Nat Commun 6:8394
19. Ramanujam PS, Hvilsted S, Ujhelyi F, Koppa P, Lörincz E, Erdei G, Szarvas G (2001) Physics and technology of optical storage in polymer thin films. Synth Met 124:145–150
20. Boyle AJ, Weems AC, Hasan SM, Nash LD, Monroe MBB, Maitland DJ (2016) Solvent stimulated actuation of polyurethane-based shape memory polymer foams using dimethyl sulfoxide and ethanol. Smart Mater Struct 25:075014
21. Kizilkaya S. Investigations of reactions of 2,3-furandions, p.113, Master Thesis, Yüzüncü Yıl Üniversitesi, February 2009
22. Çetin A, Bildirici İ (2018) A study on synthesis and antimicrobial activity of 4-acyl-pyrazoles. J Saud Chem Soc 22(3):279–296
23. Huang J, Wang KX, Chang JJ, Jiang YY, Xiao QS, Li Y (2017) Improving the efficiency and stability of inverted perovskite solar cells with dopamine-copolymerized PEDOT: PSS as a hole extraction layer. J Mater Chem A 5:13817–13822
24. El-Nahass MM, Desoky WM (2017) Investigating the structural and optical properties of thermally evaporated 1,3,3-trimethylindolino-β-naphthopyrylospiran thin films. Appl Phys A 123:517
25. Yuan Y, Giri G, Ayzner AL, Zoombelt AP, Mannsfeld SC, Chen J. Bao Z (2014) Ultra-high mobility transparent organic thin film transistors grown by an off-centre spin-coating method. Nat Commun 5:3005
26. Muhammad FF, Aziz SB, Hussein SA (2015) Effect of the dopant salt on the optical parameters of PVA:NaNO3 solid polymer electrolyte. J Mater Sci-Mater El 26:521–529
27. El-Mansy MK, Sheha EM, Patel KR, Sharma GD (2013) Characterization of PVA/CuI polymer composites as electron donor for photovoltaic application. Optik 124:1624–1631
28. Esfahani ZH, Ghanipour M, Dorranian D (2014) Effect of dye concentration on the optical properties of red-BS dye-doped PVA film. J Theor Appl Phys 8:117–121
29. Sista S, Park MH, Hong Z, Wu Y, Hou J, Kwan WL, Yang Y (2010) Highly efficient tandem polymer photovoltaic cells. Adv Mater 22: 380–383

30. Riede M, Uhrich C, Widmer J, Timmreck R, Wynands D, Schwartz G, Sundarraj S (2011) Efficient organic tandem solar cells based on small molecules. Adv Funct Mater 21:3019–3028
31. Dou L, You J, Yang J, Chen CC, He Y, Murase S, Yang Y (2012) Tandem polymer solar cells featuring a spectrally matched low-bandgap polymer. Nat Photonics 6:180
32. Wu CG, Hsieh CW, Chen DC, Chang SJ, Chen KY (2005) Low band gap-conjugated polymer derivatives. Synth Met 155:618–622
33. Demadrille R, Firon M, Leroy J, Rannou P, Pron A (2005) Plastic Solar Cells Based on Fluorenone-Containing Oligomers and Regioregular Alternate Copolymers. Adv Funct Mater 15:1547–1552
34. Kaya İ, Çöpür S, Karaer H (2017) Synthesis, characterization and electrochemical properties of poly (phenoxy-imine) s containing carbazole unit. Int J Ind Chem 8:329–343
35. Sharifi-viand A, Mahjani MG, Jafarian M (2014) Determination of fractal rough surface of polypyrrole film: AFM and electrochemical analysis. Synth Met 191:104–112
36. Passeri D, Rossi M, Tamburri E. Terranova ML (2013) Mechanical characterization of polymeric thin films by atomic force microscopy based techniques. Anal Bioanal Chem 405:1463–1478
37. Patra D, Lee J, Lee J, Sredojevic DN, White AJ, Bazzi HS, Al-Hashimi M (2017) Synthesis of low band gap polymers based on pyrrolo[3,2-d:4,5-d′]bisthiazole (PBTz) and thienylenevinylene (TV) for organic thin-film transistors (OTFTs). J Mater Chem C 5:2247–2258
38. Hou J, Chen HY, Zhang S, Chen RI, Yang Y, Wu Y, Li G (2009) Synthesis of a low band gap polymer and its application in highly efficient polymer solar cells. J Am Chem Soc 131:15586–15587